

Nonequilibrium Mechanics and Dynamics of Motor-Activated Gels

F. C. MacKintosh^{1,2,*} and A. J. Levine³¹*Department of Physics & Astronomy, Vrije Universiteit, 1081HV Amsterdam, The Netherlands*²*The Kavli Institute for Theoretical Physics, University of California, Santa Barbara, California 93106, USA*³*Department of Chemistry & Biochemistry and the California Nanosystems Institute, University of California, Los Angeles, California 90095, USA*

(Received 10 July 2007; published 8 January 2008)

The mechanics of cells is strongly affected by molecular motors that generate forces in the cellular cytoskeleton. We develop a model for cytoskeletal networks driven out of equilibrium by molecular motors exerting transient contractile stresses. Using this model we show how motor activity can dramatically increase the network's bulk elastic moduli. We also show how motor binding kinetics naturally leads to enhanced low-frequency stress fluctuations that result in nonequilibrium diffusive motion within an elastic network, as seen in recent *in vitro* and *in vivo* experiments.

DOI: 10.1103/PhysRevLett.100.018104

PACS numbers: 87.16.Ka, 62.20.D-, 87.15.La

The mechanics of living cells are largely governed by the *cytoskeleton*, a complex network of filamentous protein aggregates and various specialized proteins and enzymes that couple the filaments together and generate forces [1]. As materials, *in vitro* networks of cytoskeletal filaments have been shown to have unusual mechanical properties, including a highly nonlinear elastic response [2–6] and negative normal stresses [7]. Cytoskeletal networks *in vivo*, however, are far from equilibrium materials, due in large part to molecular motors that exert internal forces within the networks. This presents a challenge for quantitative statistical or thermodynamic modeling. Recent studies of *in vitro* networks that include molecular motors have shown nearly a 100-fold stiffening of the networks due to motor activity, as well as pronounced low-frequency, non-equilibrium fluctuations [8]. Here, we develop a model for such active gels that can explain both the strong stiffening of networks with motor activity, as well as the large nonequilibrium fluctuations at low frequencies. We also show how motor (un)binding kinetics naturally leads to a very simple and general form of stress fluctuations and diffusivelike motion, which are consistent with observed nonequilibrium dynamics in living cells [9,10]. This model can form the basis for quantitative design principles for creating synthetic polymeric materials with tunable elastic properties and musclelike activation.

Active solutions consisting of polymers and motors constitute a strikingly new kind of material that can actively change or adapt its macroscopic mechanical properties due to small-scale motor activity that drives relative sliding of polymers past each other [11–15]. In permanently cross-linked networks, however, such motor activity can produce tensile stresses [8]. This musclelike contraction is sketched in Fig. 1(a). It is well known that single semiflexible polymers stiffen under extension [16], and that this can result in macroscopic stiffening of networks under external strain [3,4,17]. This effect can also account for the observed dramatic stiffening of active networks [8,18]. Assuming an average state of tension in the network

strands due to motor activity, we can calculate the expected degree of network stiffening as follows. The tension τ in a single filament is calculated as a function of longitudinal extension ℓ as in Ref. [17], from which an effective spring constant $K = d\tau/d\ell$ is calculated. In the nonlinear regime, this increases as $K \propto \tau^{3/2}$ [3]. The network modulus is

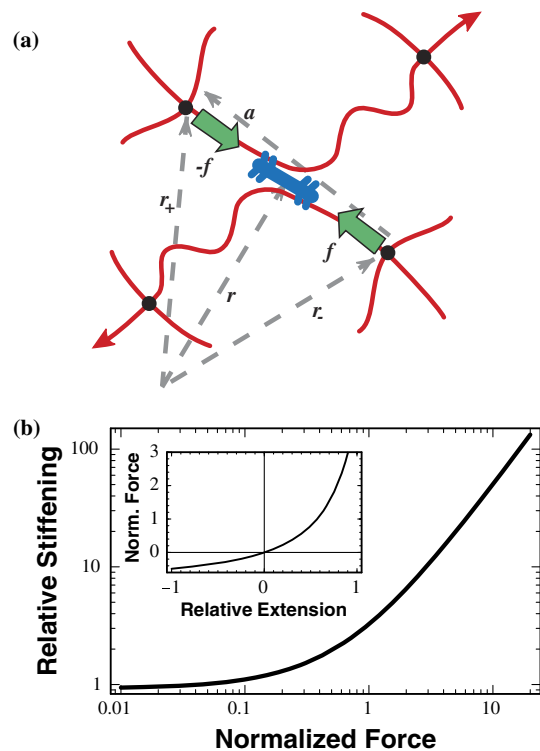


FIG. 1 (color online). (a) Schematic diagram of contractile motor activity in a network. A myosin minifilament (blue) slides two network filaments (red) past each other, generating an equal and opposite pair of forces (green arrows). (b) Plot of the predicted relative stiffening of a semiflexible network as a function of (normalized) motor-induced tension. The inset shows the nonlinear force-extension relation of a single semiflexible filament [3,4,17].

given by $G = \frac{1}{15} \rho \ell_c K$, where ρ is the density (length per volume) of polymer, and ℓ_c is the distance between cross-links [19,20]. The predicted stiffening is shown in Fig. 1(b), where the filament tension has been normalized by the characteristic tension $\tau_0 = kT \pi^2 \ell_p / \ell_c^2$ required to pull out the fluctuations on a filament of length ℓ_c in the network. Here, ℓ_p is the persistence length. For a network of actin filaments, such as in Mizuno *et al.* [8], where $\ell_p = 17 \mu\text{m}$ and $\ell_c \approx 3 \mu\text{m}$, this characteristic average tension is of order 0.1 pN, meaning that a tension of just a few pN, which is easily reached by myosin motors, can lead to the observed 100-fold stiffening of active networks.

The quasistatic picture sketched in Fig. 1(a) shows a motor (myosin minifilament) generating a pair of equal and opposite forces $\mp \vec{f}$ applied at points $\vec{r}_\pm = \vec{r} \pm \vec{a}/2$, separated by \vec{a} . We expect a to be a few microns in an *in vitro* network. Since actin filaments are not able to support compressive loads over this distance, the resulting force dipole is contractile: the points are pulled together by a sort of musclelike activity. While individual myosin motors are nonprocessive and are incapable of persistent, directed motion, they self-assemble into minifilaments, which are processive. These minifilaments still have a finite duty ratio. When they unbind, the tension is instantaneously released, as sketched in the inset of Fig. 2 [8]. Such a steplike force $f(t)$ corresponds to a power spectrum of force fluctuations that varies as ω^{-2} , proportional to the square Fourier transform of f .

As we show, this physical picture of steplike contractile forces naturally leads to nonequilibrium fluctuations that dominate only at low frequencies, as sketched in Fig. 2. Surprisingly, this generates motion that appears to be diffusive: $\langle |x(t) - x(0)|^2 \rangle \sim Dt$, but occurring in an *elastic* material. The effective diffusion constant D is controlled by motor activity and not temperature. Using well-established viscoelastic properties of cross-linked F-actin networks [19,20], we find distinct regimes of both thermal and athermal (motor-induced) fluctuations sketched in

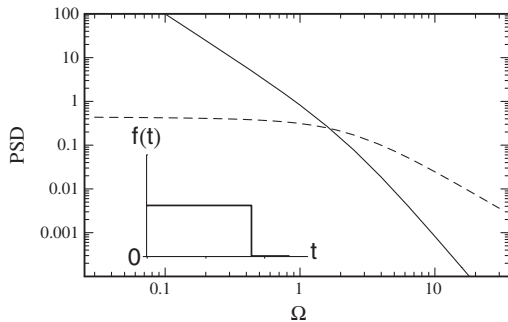


FIG. 2. The displacement power spectral density (PSD) in an active gel. Here, frequency is measured in terms of $\Omega = \omega \Gamma / B$. The thermal PSD (dashed line) shows a plateau at low frequencies. Thus, the active component of the PSD dominates at low frequencies, while the thermal PSD is expected to dominate at high frequencies. (Inset) Schematic of the time-dependent force due to molecular motor activity.

Fig. 2, which are consistent with the observations both *in vivo* [9] and *in vitro* [8].

To model the active gel we use a continuum description for a viscoelastic homogeneous and isotropic medium, but in which the motor activity couples to this medium as illustrated in Fig. 1(a). For *in vitro* networks such as in Ref. [8], the distance between cross-links, and thus a , is expected to be of order 3–10 μm . On this scale, we can model the action of a motor as the introduction of a pair of equal and opposite applied forces in the (visco-)elastic continuum. The resulting displacement field u_i at position \vec{r}_0 of the network we describe by a linear response function α_{ij} depending on position and frequency as

$$u_i(\vec{r}_0, \omega) = [\alpha_{ij}(\vec{r}_0 - \vec{r}_-, \omega) - \alpha_{ij}(\vec{r}_0 - \vec{r}_+, \omega)] f_j(\omega), \quad (1)$$

using the fact that the motor-generated forces $\mp \vec{f}$ are equal and opposite. Stability also requires that \vec{f} and \vec{a} be parallel. The response function to a point force α_{ij} can be written in terms of α_{\parallel} and α_{\perp} , where $\alpha_{ij}(\vec{r}) = \hat{r}_i \hat{r}_j \alpha_{\parallel}(r) + (\delta_{ij} - \hat{r}_i \hat{r}_j) \alpha_{\perp}(r)$.

We calculate these two response components within a two-fluid approximation, in which the cytoskeletal filaments are treated as a porous elastic network immersed in a viscous solvent [21–24]. Here, the network displacement u and solvent velocity v satisfy the coupled equations

$$0 = \mu \nabla^2 \vec{u} + (\mu + \lambda) \vec{\nabla} (\vec{\nabla} \cdot \vec{u}) + \Gamma \left(\vec{v} - \frac{d\vec{u}}{dt} \right) + \vec{f}_n, \quad (2)$$

$$0 = \eta \nabla^2 \vec{v} - \vec{\nabla} P - \Gamma \left(\vec{v} - \frac{d\vec{u}}{dt} \right) + \vec{f}_s, \quad (3)$$

where μ and λ are Lamé coefficients, η is the solvent viscosity, and the forces $f_{n,s}$ represent the forces on the network and solvent, respectively. Given a meshwork with a pore size ξ , the coupling Γ is expected to be of order η / ξ^2 . These are solved for the response of the combined system to an applied point force. The resulting response functions are given by

$$\alpha_{\parallel}(r, \omega) = \frac{1}{4\pi r G(\omega)} \left[1 + \frac{G(\omega)}{B(\omega)} \chi_{\parallel}(r\sqrt{\Omega}) \right], \quad (4)$$

and

$$\alpha_{\perp}(r, \omega) = \frac{1}{8\pi r G(\omega)} \left[1 + \frac{G(\omega)}{B(\omega)} \chi_{\perp}(r\sqrt{\Omega}) \right], \quad (5)$$

where $\chi_{\perp}(x) = 2i[1 - (1 + x\sqrt{-i})e^{-x\sqrt{-i}}]/x^2$ and $\chi_{\parallel}(x) = e^{-x\sqrt{-i}} - \chi_{\perp}(x)$. Here, G is the shear modulus and $B = \frac{2(1-\sigma)}{1-2\sigma} G$ is the longitudinal modulus, where σ is the Poisson ratio, and $\Omega = \omega \Gamma / B$. This coupling can be understood in terms of the solvent flow through the highly porous gel: rapid solvent flow through the filament mesh gives rise to large shear stresses, effectively dragging the network with the solvent. This drag prevents the large-

scale relative motion of the network and solvent beyond a range of order $\Omega^{-1/2}$. On larger length scales r or at higher frequencies ω , the drag effectively inhibits the relative motion of solvent and network so that for $r\sqrt{\Omega} \gg 1$, the combined network and solvent act as a single incompressible material [23,24], and $\chi_{\parallel,\perp}$ both vanish [Fig. 3(a)]. Here, the response of the medium is purely *transverse* (the displacement vector field is divergenceless) and is given by the generalized Oseen tensor, given by leading terms in square brackets above [24]. The corresponding volume-preserving flow response of an incompressible gel when subject to a symmetric pair of point forces is shown in Fig. 4(a).

In this incompressible case, the displacement field $u(\omega)$ of the network resulting from motor activity varies with an overall frequency dependence proportional to the ratio of the force $f(\omega)$ to the shear modulus $G(\omega)$, according to Eqs. (1)–(3). Thus, we find for the model illustrated in Fig. 1(a) that $\langle |u(\omega)|^2 \rangle \propto \langle |f(\omega)|^2 \rangle / |G(\omega)|^2 \propto |\omega G|^{-2}$. Cross-linked biopolymer networks typically exhibit a constant or weakly frequency-dependent elastic regime as a function of frequency. Here, we expect to see $\langle |u(\omega)|^2 \rangle \propto$

ω^{-2} , which is consistent with recent displacement fluctuations observed in cells [9], and which corresponds to diffusive motion. At higher frequencies, such networks typically exhibit a power-law increase in the shear modulus with frequency [19,20,23], in which $G \propto \omega^{3/4}$. In this frequency regime stain fluctuations in the active gel take the form $\langle |u(\omega)|^2 \rangle \propto \omega^{-7/2}$, as shown in Fig. 2. For comparison, the equilibrium thermal fluctuations for such a network are shown as the dashed line. At low frequencies the motor-driven fluctuations will dominate over the ever-present thermal fluctuations, consistent with the results of both Lau *et al.* [9] and Mizuno *et al.* [8].

Since biopolymer and cytoskeletal networks are generically porous with pore sizes of order $1 \mu\text{m}$, they can deform *compressibly*. This density mode, however, is strongly suppressed by drag at high enough frequencies. The loss of the density mode at high frequencies is illustrated in Fig. 3(a), where the effects of finite compressi-

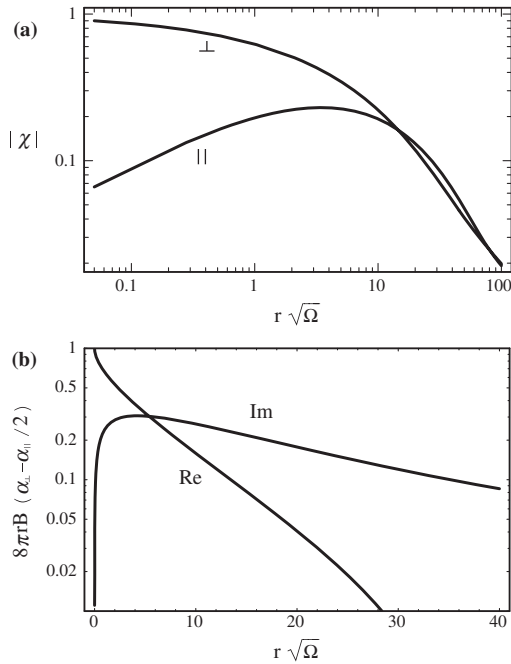


FIG. 3. (a) Graphs of the spatial dependence of the longitudinal parts of the parallel (\parallel) and perpendicular (\perp) response functions [Eqs. (2) and (3)]. The effect of compression of the network on the response functions can be reduced to a universal form when plotted against the dimensionless quantity $r\sqrt{\Omega} = r\sqrt{\omega\Gamma/B}$, demonstrating the diffusive nature of the propagation of the network density mode. (b) The effect of network compression can be isolated in experimental data by examining the difference in the parallel and perpendicular response functions given in Eq. (4). Here we plot the predicted form of the real (Re) and imaginary (Im) parts of that difference vs the dimensionless variable $r\sqrt{\Omega}$.

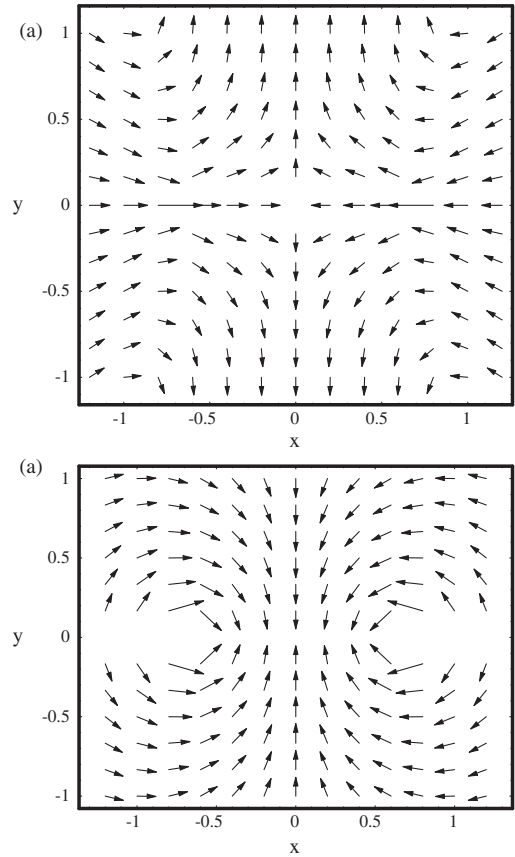


FIG. 4. (a) The displacement vector field of an incompressible network shown in a plane passing through the two force centers for a contractile motor acting at the origin. The forces are applied symmetrically at points $(\pm 3/4, 0)$ and are each directed towards the origin. (b) The network displacement field for the compression mode shown in the limit of low frequency or weak hydrodynamic coupling ($\Gamma \rightarrow 0$). Again, the forces are applied symmetrically at points $(\pm 3/4, 0)$ and are each directed towards the origin. The resulting displacement field induces network density variations in the material.

bility, represented by $\chi_{\parallel,\perp}$, vanish at high frequency. Although the basic physics of these effects have been discussed before for both flexible polymer systems [21,22] and semiflexible biopolymer systems [23,24], there has been no direct experimental observation of these compressibility effects in porous biopolymer systems.

We can isolate the effects of the network compressibility by the examining the combination

$$\alpha_{\perp}(r, \omega) - \frac{1}{2}\alpha_{\parallel}(r, \omega) = \frac{[\chi_{\perp}(r\sqrt{\Omega}) - \frac{1}{2}\chi_{\parallel}(r\sqrt{\Omega})]}{8\pi rB(\omega)}, \quad (6)$$

which is plotted in Fig. 3(b). This measurable combination of response functions strictly vanishes in the incompressible limit. This, along with the specific combined r and ω dependence, may permit the first direct measurement of compressibility effects that are expected to be characteristic of biopolymer or cytoskeleton networks. Furthermore, the flow or displacement field corresponding to this compressible mode [shown in Fig. 4(b) in the limit $\Gamma \rightarrow 0$] strongly differ from the case of an incompressible system [Fig. 4(a)]. Here, the *longitudinal* (irrotational displacement field) contributions to the response function are $\alpha_{\parallel}^{(L)} = 0$ and $\alpha_{\perp}^{(L)} = 1/(8\pi rB)$. The difference in spatial structure of these strain fields may also be used to experimentally identify the effects of compression.

To consider the effect of multiple contractile events within the medium, we can represent the resulting displacement field at the origin u_i by a sum

$$u_i = \sum \Delta\alpha_{ij}(\vec{r}, \vec{a})\hat{a}_{jf}, \quad (7)$$

where $\Delta\alpha_{ij}(\vec{r}, \vec{a}) = \alpha_{ij}(\vec{r} - \vec{a}/2) - \alpha_{ij}(\vec{r} + \vec{a}/2)$ is the response to a contractile force pair. We suppress the frequency dependence. This sum represents the combined effect of temporally uncorrelated contractile events occurring homogeneously throughout the medium. This assumption remains valid provided that the events rarely occur with a separation of order $a \sim \ell_c$ during the typical processivity time t_0 . Such a sum or average has been performed in calculating the fluctuation spectrum in Fig. 2 for the case of an incompressible network. In this case the scaling described above is a good approximation.

This model shows how motor activity within a semiflexible gel, together with the well-established nonlinear response of such networks, leads to a strong stiffening of the network, and that this stiffening increases more than linearly with the motor force. This can account for the recently observed nearly 100-fold network stiffening with motor forces of order 1–10 pN [8]. Furthermore, the (un)binding kinetics of the motors naturally leads to a specific characteristic time dependence of the force fluctuations in active gels. Given a finite processivity time t_0 over which minifilaments remain bound and generate force, the unbinding results in $1/\omega^2$ force fluctuations for frequencies $\omega > 1/t_0$. This spectrum is a direct result of the expected

sharp time dependence of motor unbinding and is insensitive to slow variations of force during motor motion. For frequencies $\omega > 1/t_0$, the divergence of the force spectrum will be suppressed. Our model is for uncorrelated motor activity, in that the total fluctuations can be represented as a sum of independent fluctuations due to individual motor force generation and unbinding. At sufficiently high motor densities, one might expect cooperativity of motor activity, whose consequences can be studied in extension of the present model.

This work was supported in part by the (Netherlands) Foundation for Fundamental Research on Matter (FOM), NSF Materials World Networks (Grant No. DMR-0354113), and the NSF through the Kavli Institute for Theoretical Physics. The authors thank J. Crocker, A. Grosberg, A. Lau, T. Lubensky, D. Mizuno, M. Rubinstein, and C. Schmidt for helpful discussions.

*fcm@nat.vu.nl

- [1] B. Alberts *et al.*, *Molecular Biology of the Cell* (Garland, New York, 1994), 3rd ed.
- [2] F.C. MacKintosh and P.A. Janmey, *Curr. Opin. Solid State Mater. Sci.* **2**, 350 (1997).
- [3] M.L. Gardel *et al.*, *Science* **304**, 1301 (2004).
- [4] C. Storm *et al.*, *Nature (London)* **435**, 191 (2005).
- [5] A.R. Bausch and K. Kroy, *Nature Phys.* **2**, 231 (2006).
- [6] O. Chaudhuri, S.H. Parekh, and D.A. Fletcher, *Nature (London)* **445**, 295 (2007).
- [7] P.A. Janmey *et al.*, *Nat. Mater.* **6**, 48 (2007).
- [8] D. Mizuno, C. Tardin, C.F. Schmidt, and F.C. MacKintosh, *Science* **315**, 370 (2007).
- [9] A.W.C. Lau *et al.*, *Phys. Rev. Lett.* **91**, 198101 (2003).
- [10] C. Brangwynne, F.C. MacKintosh, and D.A. Weitz, *Proc. Natl. Acad. Sci. U.S.A.* **104**, 16128 (2007); C. Brangwynne *et al.*, arXiv:0709.2952.
- [11] T.B. Liverpool, A.C. Maggs, and A. Ajdari, *Phys. Rev. Lett.* **86**, 4171 (2001).
- [12] L. Le Goff, F. Amblard, and E.M. Furst, *Phys. Rev. Lett.* **88**, 018101 (2001).
- [13] D. Humphrey *et al.*, *Nature (London)* **416**, 413 (2002).
- [14] T.B. Liverpool, *Phil. Trans. R. Soc. A* **364**, 3335 (2006).
- [15] K. Kruse *et al.*, *Eur. Phys. J. E* **16**, 5 (2005).
- [16] C. Bustamante *et al.*, *Science* **265**, 1599 (1994).
- [17] F.C. MacKintosh, J. Käs, and P.A. Janmey, *Phys. Rev. Lett.* **75**, 4425 (1995).
- [18] G.H. Koenderink *et al.* (unpublished).
- [19] F. Gittes and F.C. MacKintosh, *Phys. Rev. E* **58**, R1241 (1998).
- [20] D.C. Morse, *Macromolecules* **31**, 7044 (1998).
- [21] F. Brochard and P.G. de Gennes, *Macromolecules* **10**, 1157 (1977).
- [22] S.T. Milner, *Phys. Rev. E* **48**, 3674 (1993).
- [23] F. Gittes *et al.*, *Phys. Rev. Lett.* **79**, 3286 (1997); B. Schnurr, F. Gittes, F.C. MacKintosh, and C.F. Schmidt, *Macromolecules* **30**, 7781 (1997).
- [24] A.J. Levine and T.C. Lubensky, *Phys. Rev. Lett.* **85**, 1774 (2000).